Optical Materials 60 (2016) 38–44

Contents lists available at ScienceDirect

Optical Materials

journal homepage: www.elsevier.com/locate/optmat

Single Brillouin frequency shifted S-band multi-wavelength Brillouin-Raman fiber laser utilizing fiber Bragg grating and Raman amplifier in ring cavity

A.H. Reshak [a, c, *], N.A.M. Ahmad Hambali [b], M.M. Shahimin [d], M.H.A. Wahid [b], Nur Elina Anwar [b], Zeyad A. Alahmed [e], J. Chyský [f]

[a] New Technologies – Research Centre, University of West Bohemia, Univerzitni 8, 306 14 Pilsen, Czech Republic
[b] Semiconductor Photonics and Integrated Lightwave System (SPILS), Tun Abdul Razak Laser Lab Laboratory (TAReL), School of Microelectronic Engineering, Universiti Malaysia Perlis (UniMAP), Pauh Putra Main Campus, Jalan Arau-Changlun, 02600 Arau, Perlis, Malaysia
[c] Center of Excellence Geopolymer and Green Technology, School of Material Engineering, University Malaysia Perlis, 01007 Kangar, Perlis, Malaysia
[d] Department of Electrical and Electronic Engineering, Faculty of Engineering, National Defence University of Malaysia (UPNM), Kem Sungai Besi, 57000 Kuala Lumpur, Malaysia
[e] Department of Physics and Astronomy, College of Science, P.O. Box 2455, King Saud University, Riyadh 11451, Saudi Arabia
[f] Department of Instrumentation and Control Engineering, Faculty of Mechanical Engineering, CTU in Prague, Technicka 4, 166 07 Prague 6, Czech Republic

ARTICLE INFO

Article history:
Received 16 October 2015
Received in revised form
16 June 2016
Accepted 8 July 2016

Keywords:
Multi-wavelength
S-band
Fiber Bragg grating
Raman amplifier
Raman gain
Brillouin gain
Ring cavity

ABSTRACT

This paper is focusing on simulation and analyzing of S-band multi-wavelength Brillouin–Raman fiber laser performance utilizing fiber Bragg grating and Raman amplifier in ring cavity. Raman amplifier-average power model is employed for signal amplification. This laser system is operates in S-band wavelength region due to vast demanding on transmitting the information. Multi-wavelength fiber lasers based on hybrid Brillouin–Raman gain configuration supported by Raman scattering effect have attracted significant research interest due to its ability to produced multi-wavelength signals from a single light source. In multi-wavelength Brillouin–Raman fiber, single mode fiber is utilized as the nonlinear gain medium. From output results, 90% output coupling ratio has ability to provide the maximum average output power of 43 dBm at Brillouin pump power of 20 dBm and Raman pump power of 14 dBm. Furthermore, multi-wavelength Brillouin–Raman fiber laser utilizing fiber Bragg grating and Raman amplifier is capable of generated 7 Brillouin Stokes signals at 1480 nm, 1510 nm and 1530 nm.

1. Introduction

Recently, multi-wavelength fiber laser has attracted considerable interests due to their potential applications such as multiplexing, optical frequency metrology, optical frequency metrology, optical signal processing, frequency shifting, dense wavelength division multiplexing (DWDM) optical communication and data transmission amplification [1]. Desires for multi-wavelength sources consist of stable multi-wavelength peak power, low threshold power, high signal-to-noise ratio (OSNR), and flattening [2]. The biggest attention of multi-wavelength fiber laser is the stimulated Brillouin scattering (SBS) that has emerged to produce Brillouin fiber laser (BFL) and its applications. The BFL is created by sources that are equipped for creating narrow linewidth Brillouin laser. A few configurations have been utilized as a part of the BFL to produce multi-wavelength operation as reported in Ref. [3].

Alternatively, the multi-wavelength Brillouin-Raman fiber lasers (MWBRFLs) is another approach to produce multiwavelength whereby Raman amplifier is used to increase the number of Brillouin Stokes (BS) signals. The MWBRFLs has remarkable advantages such as room-temperature stable operation at room temperature, extremely broad band operational region relative to the availability of Raman pumps lasers at the corresponding wavelength and simplicity [4]. Raman gain uses the principle of Raman scattering to amplify optical signals.

Another approach to the generation of multi-wavelength fiber

* Corresponding author. New Technologies – Research Centre, University of West Bohemia, Univerzitni 8, 306 14 Pilsen, Czech Republic.
E-mail addresses: maalidph@yahoo.co.uk, azuramalini@unimap.edu.my (A.H. Reshak).

http://dx.doi.org/10.1016/j.optmat.2016.07.008
0925-3467/

laser is the integration of Raman gain, due to spontaneous Raman scattering, and Brillouin gain due to SBS in single resonator. The main advantage of Raman amplification is they can work in any wavelength band. Although, the (SBS) and stimulated Raman scattering (SRS) can be interfering in coherent optical communication systems they do serve many useful applications [5].

There are several different methods proposed for generation of the MWBRFLs as reported in Refs. [6,7]. In these papers, they are demonstrated of the MWBRFL utilizes the reverse S-shaped laser cavity technique. Raman pump (RP) is set at 1480 nm wavelength to provide Raman amplification in the dispersion compensating fiber (DCF) to amplify the BP signal. The structure generates 35 outputs BS signals with average channel peak power of 1.11 mW at BP signal power and wavelength of 6.3 mW at 1580 nm respectively, with RP power of 891.25 mW in the L-band wavelength region. They achieved a tuning range of 25 nm, from 1570 nm to 1595 nm of BP wavelength. However, all the above mentioned papers only focus on a multi-wavelength BS signals that operated at C-band and L-band wavelength region. Furthermore, the reverse-S-shaped fiber section has higher insertion loss. The S-band MWBRFLs with 20 GHz signals spacing has been demonstrated [8]. For this laser system, tuning range between 1490 nm and 1530 nm is designed with a 7.7 km long dispersion compensating fiber (DCF) in the simple ring cavity. Meanwhile, the S-band MWBRFLs distributed Bragg reflector fiber laser has been experimentally demonstrated in Ref. [9]. The Brillouin Stokes (BS) signals is achieved with two Raman pump (RP) at wavelength of 1420 nm and fiber Bragg grating (FBG) is used as a reflector. However, these two laser configuration focused on linear cavity and only 6 BS signals is produced.

In communication system, C-band and L-band region has been introduced to provide higher demanding of quick data transmission communication using wavelength to range of 1530 nm–1565 nm [10] and 1565 nm–1625 nm, respectively. However, due to enormous demanding on transmitting the information in fastest mode, it is require expanding the communication windows into S-band wavelength region (1460 nm–1530 nm). The S-band wavelength region also known as short wavelength has comparable attenuation characteristics in standard single mode fiber (SMF) than C-band (1530 nm–1565 nm) and L-band (1565 nm–1625 nm) wavelength region [11]. Moreover, sensitivity to micro-and macrobending losses in the S-band is much lower compared with C-band and L-band region [12]. Furthermore, S-band has lower dispersion in silica fiber compared in the L-band wavelength [13].

In this paper, the general configuration of the MWBRFLs utilizing FBG and Raman amplifier are simulated. We proposed additional enhancement in the previously reported configuration of a reverse-S-shaped fiber section. The reflecting FBG has the ability to functions in the similar technique as does the reverse-S-shaped fiber section but with higher insertion loss [6,7]. However, the proposed configuration is focus on operating in S-band wavelength region. The MWBRFL utilizing FBG has the ability to generate maximum 7 BS signal. This paper is devoted to investigate the performance of the MWBRFL utilizing Brillouin and Raman gain prior to produce BS signals in SMF. The most BS signals is generated at 14 dBm of Raman pump (RP) power and average peak power is produced around 35 dBm to 45 dBm. In addition, the MWBRFL has a good ability to operate in a stable condition at room temperature [4]. At room temperature, the MWBRFL has the competency to operate with abstaining from the adverse influence of self lasing cavity mode [14].

2. Configuration

The simulation layout and illustration of S-band multi-wavelength BRFL utilizing fiber FBG in a simple ring configuration is shown Fig. 1, respectively. It consists of single mode fiber (SMF), Raman fiber, optical circulator (Cir), optical pump coupler, optical bidirectional coupler, optical spectrum analyzer (OSA), and external tunable laser source (TLS), FBG and bidirectional Raman amplifier-average power model. SMF is act as Brillouin-Raman gain media. SMF has attenuation of 25 dB and a dispersion value of 16.75 ps/nm/km. The BP signal with a linewidth of approximately 200 kHz is provided by utilizing an external TLS. The narrow linewidth of BP signal amplified by bidirectional Raman amplifier is used in order to create stimulated Brillouin Scattering (SBS) effect and the subsequent to produce narrow linewidth multiple wavelengths lasing signals. The TLS from a 1460 nm–1530 nm operating wavelength with a maximum output power of 20 dBm is used as a BP signal and Brillouin gain. An optical circulator is used to allow the optical signal to propagate in the anticlockwise direction and circulate in a clockwise direction. A bidirectional optical coupler with different coupling ratios provides as output medium is connected to an optical spectrum analyzer (OSA) that is used for extracted the results and monitored by an OSA with 0.015 nm of bandwidth resolution. An optical pump coupler is used to combine the BP signal and pump signal. A FBG with 90% reflectivity is used to reflect the signals with high efficiency and to produce lower loss. Meanwhile, bidirectional Raman amplifier-average power model with wavelength fixed at 1425 nm is used to provide Raman signal and Raman amplification. The bidirectional Raman amplifier average power model is assembled with 10 km length of fiber with attenuation of 0.2 dBm/km and effective interaction area of 72 μm^2. The Raman amplification happens in the SMF, which is used to amplify the injected BP signal and used Raman scattering principle to amplify the BP signal. Raman signal have wavelength stability of $\pm$100 MHz/h, linewidth of <2 nm and output power stability of <1%. Moreover, the Raman gain spectrum has a bandwidth of approximately 6 THz.

To generate the output signal from the MWBRFL, the BP signal form TLS and Raman signal from Raman pump (RP) are injected to the optical coupler. The combined signal is then propagated to port-1 through port-2 of optical circulator. It is travel in anti-clockwise direction and directed to the FBG. FBG allows certain amount of signals to propagate back in clockwise direction from reflection process. Moreover, the BP signal is propagated into the bidirectional Raman amplifier-average power model and SMF. The bidirectional Raman-amplifier-average power model has a function that is used to provide Raman gain and amplify the signals after being reflected by the FBG. Afterwards, BP signal are amplified by Raman gain and Raman amplification also occurs in the SMF. As the BP signal pass through SMF, first-order BS signal and anti-Stokes signal that has been generated from spontaneous scattering and amplified through Raman amplifier-average power model [15]. Interaction between the BP signal and acoustic waves in SMF causes SBS effect. This condition leads to generate the backward propagation frequency shifted light that namely as BS signal. This BS signal is down shifted in frequency due to Doppler shift associated with grating moving at acoustic velocity [16]. The first-order BS signal is downshifted at ~0.08 nm which is opposite direction from the BP signal and propagated to the optical coupler for observation. The SBS effects in a SMF allow to produce the multi-wavelength generation with constant spacing at ~0.08 and narrow linewidth at room temperature [17]. Meanwhile, anti-Stokes signal are generated through four wave mixing (FWM) between co-propagating pump and BS signal as depicted in Fig. 2. The first-order BS signal is created when acquires SBS threshold condition. The SBS threshold condition can be define as the input pump power at which the back scattered power begins to increase rapidly the pump wave initiates to be depleted [18]. Then, first-order BS signal grows to reach threshold condition, it act as a new BP signal for

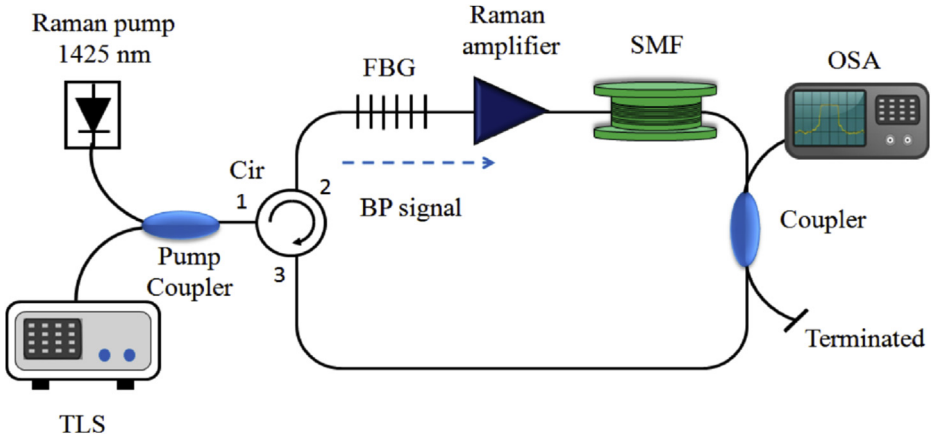

Fig. 1. Illustration of the S-Band MWBRFL utilizing FBG and Raman amplifier.

second BS signal and back scattered. When the second BS signal grows and reach threshold condition, it act as new third BP signal and back scattered. The second-order of BS signal has be generated similar condition when fist-order BS signal is propagated back into the FBG and SMF. Same process repeated to generation higher orders BS signal until the Raman and Brillouin gain is not sufficient to compensate the cavity loss [19]. At every stage, BP signal and BS signal are amplified by Raman gain and reflected by FBG. The behaviour of the MWBRFL signals is observed throughout the simulation output. At 10 km of the SMF lengths, five different output coupling ratios of 50%, 60%, 70%, 80% and 90% are simulated for the optimization. Furthermore, the outputs at each output coupling ratio are observed by optical spectrum analyzer (OSA). An average power of Raman amplifier model is employed to minimize the simulation time prior to solve its differential equations [20]. Fig. 3 indicates the list of parameters of Raman amplifier-average power model that is used in simulation.

Theoretically, SBS and SRS effect should be calculated by solving the couple wave equation for the signal I_S, Raman pump signal I_R and Stokes wave I_S intensities as in equations (1) and (2) [21].

$$\frac{dIs}{dz} = -g_B IIs + \alpha_s I_s \cdot g_R I_s I_R \tag{1}$$

and

$$\frac{dI}{dz} = -g_B IIs + \alpha I_s - g_R II_R \tag{2}$$

where g_B, g_R, are gain coefficients of Brillouin and Raman, respectively. α_s and α are fiber loss coefficients for the Stokes wave and the signal, respectively. Reflected Brillouin Stokes wave propagates in the opposite direction of the signal wave from z = L to z = 0 (L is the fiber length) [21].

Meanwhile, the Raman gain, G_R of fiber length L is obtained as per equation in (3). It depends on the pump intensity, the effective Raman gain coefficient and the polarization state [21].

$$G_R = 4.34\left[g_R L e_{ff}\frac{P_o}{K} - \alpha_s L\right] \tag{3}$$

where, K is polarization factor, L_{eff} is effective length, $P_p^{in} = P_o$ is input power, α_s is fiber loss at frequency $\omega_s$and $g_R$is Raman gain coefficient in a fiber ($W^{-1}m^{-1}$). Practically, Raman gain coefficient depends on the composition of the fiber core.

In this work, Raman gain is used in conjunction with SBS, Raman Scattering process and FBG reflectivity to expedite the BS process. The SBS and Raman scattering is a nonlinear phenomenon are related to the interaction between photons and phonons. Raman scattering arises due to interaction of light with the vibrational

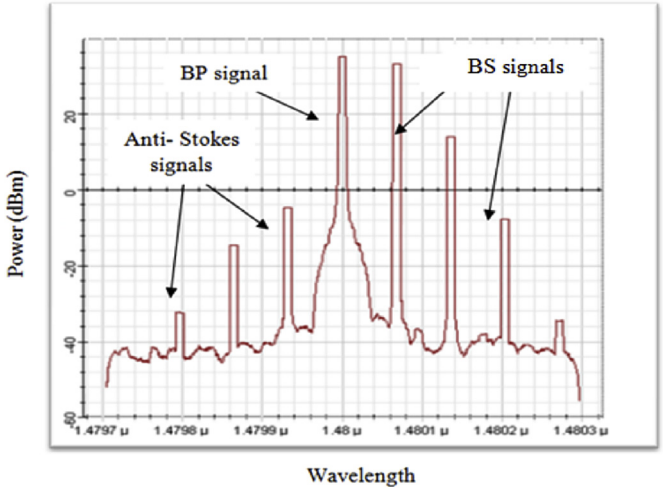

Fig. 2. Output spectra of the MWBRFL at 1480 nm of BP wavelength, RP power at 14 dBm and 60% output coupling ratio.

Disp	Name	Value	Units	Mode
☑	Length	10	km	Normal
☐	Attenuation data type	Constant		Normal
☐	Attenuation	0.2	dB/km	Normal
☐	Attenuation file	FiberLoss.dat		Normal
☐	Effective area data type	Constant		Normal
☐	Effective interaction area	72	um^2	Normal
☐	Effective interaction area f	EffectiveArea.dat		Normal
☐	Raman gain type	Raman gain		Normal
☐	Raman gain peak	1e-013		Normal
☐	Raman gain reference pu	1000	nm	Normal
☐	Gain X frequency	RG.dat		Normal

Fig. 3. List of parameter for Raman amplifier-average power model from Optisystem software.

modes of the molecules in a medium. In other words, Raman scattering can be described as light scattering from optical phonons. Brillouin scattering is the scattering of light from refractive index variation caused by sound waves attributed to propagating pressure (and thus density) waves. Scattering of light from acoustic phonons can also be considered as Brillouin scattering. The SMF that is used to generate of Brillouin gain also be utilized to generate the Raman gain. When a BP signal is lunched into an SMF, Raman scattering, normally referred to as spontaneous Raman Scattering occupy, it leads to Stimulated Raman Scattering. At this condition. The BP signal and BS signal wavelength are coherently coupled by the SBS and Raman Scattering process, respectively. Raman Scattering process is caused by interaction of light with vibrational modes of molecules of lattice vibrations of crystals [22]. Raman Scattering is an inelastic process that occurs when a pump photon, excites a molecule up to a virtual level (intermediate state). A molecule finally drops to a lower energy level and emitting a signal photon as depicted in Fig. 4. There are two types of Raman Scattering which is Spontaneous and Stimulated. Raman scattering is a third-order nonlinear process.

In practically, spontaneous Raman scattering can be observed in any material. Spontaneous Raman scattering occurs if the intensity of the incident field is below a threshold level [24]. In this condition photon are scattered into random direction. In this situation, a signal photon reduced energy, created spontaneously when a pump photon of energy is lift to a virtual energy level [23]. The absorption process will be continued and permitting multi-photon Raman scattering occur in the final state. Multi-photon transitions happen in stimulated Raman-scattering (SRS) process. SRS only occur when the pump power exceeds a certain threshold level. The process of Raman scattering in the SMF is illustrated in Fig. 4. This effect is due to a transition of incident photon energy by a molecule from ground energy level (E1) to the virtual energy level (E3), from which it immediately returns to a final energy level (E2) or molecular vibration level emitting a photon with different energy. The molecular vibration level is a vibration mode of the material. The energy difference between the ground energy level (E1) and the final level (E2) of the molecule is changed to a phonon which is a vibration mode of the material. An optical phonon of energy (E2-E1) is left behind. The phonon frequency is given as $v = (E2\text{-}E1)/h$, where h is the Planck's constant. In this work, the frequency of the BP signal and BS signal are donated by v_p and v_s, respectively. The molecule at the vibration state is stimulated by the signal, thus emitting a photon of the similar frequency and direction as the incoming signal. At this condition, Raman amplification is allowed to carry out its role in the SMF and used to increases the number BS signals in the MWBRFL.

3. Results and discussion

In order to compare the number of BS signals characteristic of the RP power and output coupling ratio, the graph in Fig. 5 is plotted. The number of BS signals are continuously increase with the increasing of RP power and output coupling ratio. In these cases, output coupling ratio is varied from 50% to 90% and RP power is varied from 6 dBm to 14 dBm. Meanwhile, BP power and wavelength are at 20 dBm and 1480 nm, respectively. From the plotted graphs in Fig. 5, at RP power of 14 dBm, 90% output coupling ratio and 1480 nm of BP wavelength, respectively are identified as the optimum parameters which is capable to produce the maximum BS number. At optimum RP power of 14 dBm, it is found that the MWBRFL is capable to enhance 7 BS signals at 70%, 80% and 90% output coupling ratio, which is attributed to the higher Raman gain [25]. At this condition, energy of the RP is sufficient to drive up the Brillouin component, hence 7 BS signals are generated optimum RP power. Moreover, when output coupling is diverse from 50% to 90%, the MWBRFL is experience the increases of the energy inside the cavity [26]. Consequently, at 50% output coupling ratio, number BS signals produced is lower compared to the number BS signals produced at 70%, 80% and 90% output coupling ratio. At 50% output coupling ratio, only 2, 3, 4 and 6 BS signals are obtained with RP power of 6 dBm, 10 dBm, 12 dBm and 14 dBm, respectively. When the MWBRFL is extended further to the increment of the RP power, the combined effect of SBS, SRS and energy inside the cavity gets stronger as more number of photons become available to be exploited. However, further extending the output coupling ratio from 50% to 90% requires higher RPP to overcome the cavity loss. At lower RP power of 6 dBm, 2, 3, 4, 5 and 4 BS signals are produced at output coupling ratio of 50%, 60%, 70%, 80% and 90%, respectively. Further clarification of the generated MWBRFL spectra of 1480 nm of BP wavelength, RP power at 14 dBm and 60% output coupling ratio are shown in Fig. 2. The output optical spectra profile presence the combination of the BP signal and anti-Stokes signal that generated from stimulated Brillouin scattering and FWM effect, respectively. Basically, Brillouin and Raman scattering are cooperated together in the MWBRFL. In the scattering process, the frequency of incident light to be shifted to a lower value, this components are identified as BS signal. Meanwhile, the components which are shifted to higher frequencies are identified as anti-Stokes signal. In the ring cavity MWBRFL, the BP signal and BS signal is propagating oppositely. Thru this process, it stimulated the degenerate and non-degenerate FWM processes [27]. The wavelength signal spacing between the BS signal and BP signal is found to be ~0.08 nm, comparable to frequency spacing of ~10 GHz and narrow linewidth feature. With very narrow linewidth of MWBRFL,

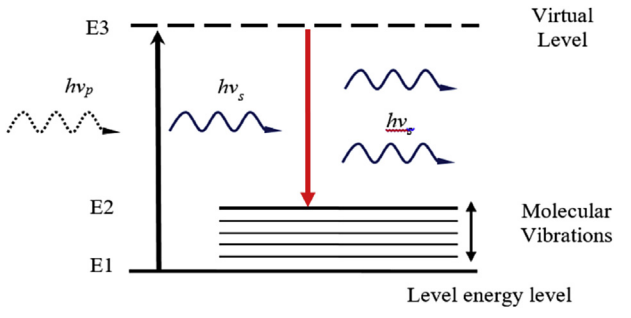

Fig. 4. Schematic energy diagram of Stimulated Raman Scattering in the SMF fiber [23].

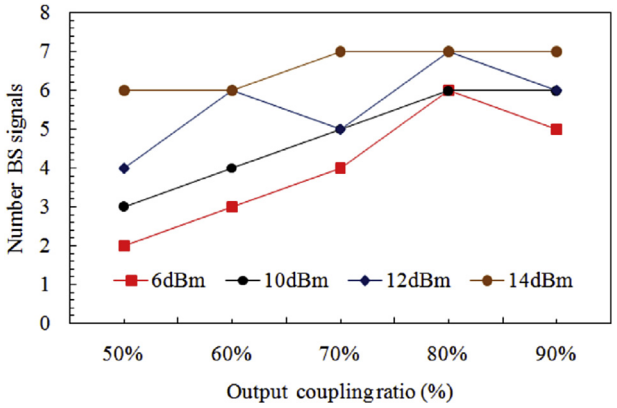

Fig. 5. Coupling ratio versus number BS signals at different RP power.

that made it of interest in several applications especially for optical communication. Fig. 2 shows that the first-order BS signal occurred as BP power exceed the SBS threshold. At this condition, maximum of the BP power is transferred to the first-order BS signal. It is worth to be highlight that the MWBRFL spectra shows the peak power of the first-order BS signal and anti-stokes signal is much lower than the second-order BS signal and anti-Stokes signal, respectively [28]. This is because the weak BP signal is then mixed with the second-order BS signal and anti-Stokes signal, thus produced a lower first-order BS signal and anti-Stokes signal as reported in Ref. [27].

Optical losses in the optical fiber can be relates to absorption, Raman scattering and Brillouin scattering. This losses is effected the performance and degraded the output signal significantly. Raman scattering and Brillouin scattering can lead to produce high losses by the transfer of energy from a wavelength to another wavelength at high pump power [31]. In SMF, basically there are two dissimilar physical mechanisms to clarify the interference process between the laser light (BP signal) and Stokes wave which leads to acoustic wave generation. These mechanisms are electrostriction and optical absorption. The electrostriction mechanism is the propensity of materials to become denser when very high power of laser light is injected inside the gain medium. Meanwhile, the scattering of light from sound waves where it is approach by modify of optical energy to thermal. This condition is followed by heating and then medium density variations [16]. This process is known as optical absorption mechanism. As illustrated in Fig. 4, the multiple BS signals are produced by scattering of light from sound waves which has been stimulated by the interference of the BP signal and Stokes fields through the process of electrostriction [16,29]. At the same time, BP signals are amplified by Raman gain. In generally, absorption of light causes thermalization of the optical energy that contributes to high temperature and density variation inside the SMF [16]. Typically, this situation occurs when the absorption coefficient in SMF is very high [30,31] When the value of RP powers are increases as presented in Fig. 5, the BS signals acquire different gains values through the SRS and SBS process. Furthermore, at high RP power, the absorption of light caused thermalization of the optical energy leading to generate high temperature and medium density variation [16].

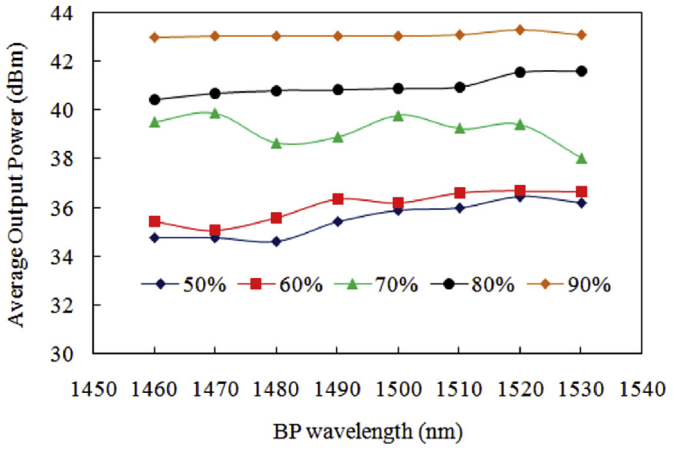

Fig. 6. Average output power against BP wavelength at 14 dBm of RP power.

To obtain the average output power of the MWBRFL, the BP wavelength is varied within 1560 nm–1530 nm with different output coupling ratio of 50%, 60%, 70% 80% and 90% as plotted in Fig. 6. Meanwhile, RP power and BP power is fixed at 14 dBm and 20 dBm, respectively. Obviously, the average output power for BP wavelength is increases with the increment of the output coupling ratio. The increment of average output power is inline with the increment of output coupling ratio from 10% to 90%. At optimum output coupling ratio of 90%, average output power which is around 43 dBm over 20 nm bandwidth are generated with best flatness. The average output power variations is found to be within ±0.5 dBm at 90% of output coupling ratio. Thus, flatness of the average output power across S-band wavelength region is obtained at 90% of output coupling ratio. This excellent flatness and stability partly owes of the optimum energy inside the ring cavity. Meanwhile, average output power around 35.5 dBm, 35.1 dBm, 39.2 dBm and 41.0 dBm are produced at 50%, 60%, 70% and 80% output coupling ratio, respectively. Above the optimum output coupling ratio, the average output coupling ratio will be decreased and the cavity loss is also increased as reported in Ref. [32].

Fig. 7 shows the value of number of BS signals at different RP power and BP wavelength. This graph illustrated that as the Raman pump power increase, the number of BS signals also increased. The red-colour line across the graph shows the average number of BS signals that produced at each value of RP power. At RP power of 14 dBm, it shows that the MWBRFLs system has the ability to produce average 7 BS signals within 1460 nm–1530 nm. The

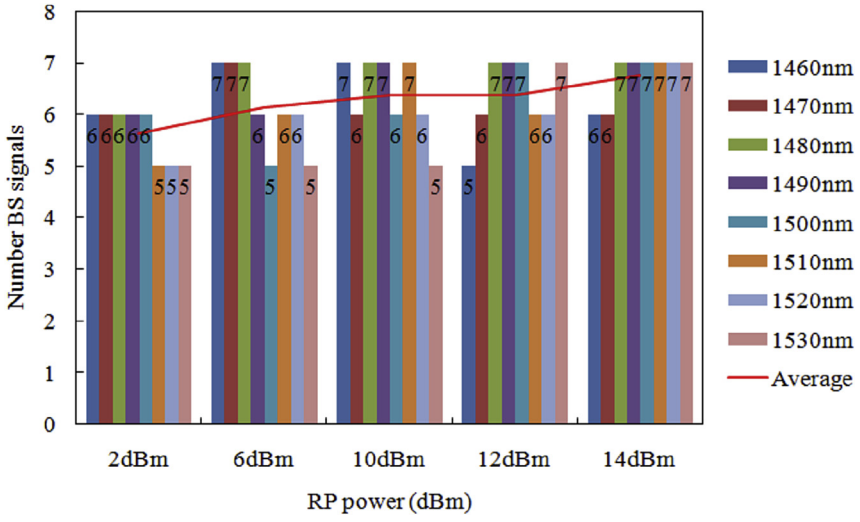

Fig. 7. Number BS signals versus RP power at different BP wavelength.

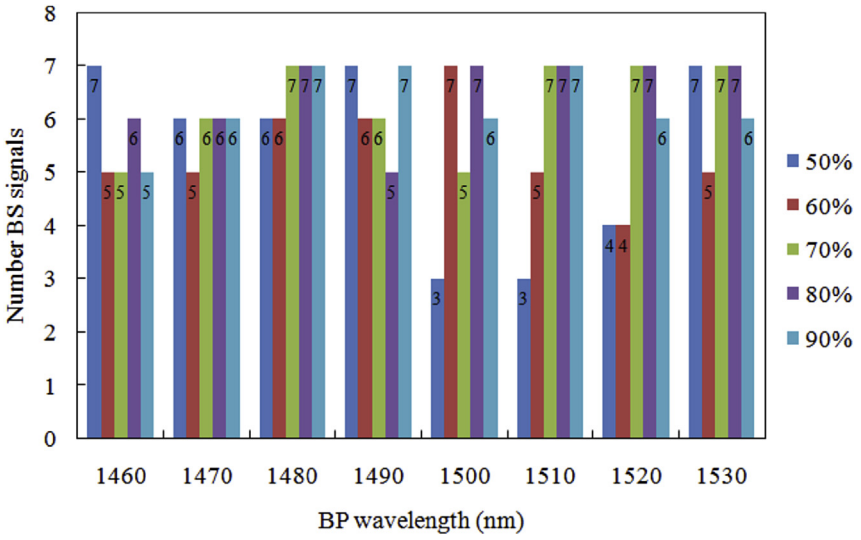

Fig. 8. Number of BS signals versus BP wavelength at different output coupling ratio.

interaction between gain medium, BP signals and RP power led to increment of Raman gain that has a direct impact on the quality of BS signals in terms of number BS signals within S-band wavelength region. Moreover, Raman gain is broadened around 1480 nm–1530 nm to produced higher number BS signals. At 2 dBm, 6 dBm, 10 dBm, 12 dBm and 14 dBm of RP power, average BS signals around 5 and 6 are produced.

Finally, in order to further analyze the output coupling ratio effect on S-band wavelength region, the graph of the number of BS signals versus BP wavelength is plotted in Fig. 8. From the graph, higher number of BS signals are obtained at 70%, 80% and 90% output coupling ratio. Meanwhile, higher number of BS signals are generated at BP wavelength of 1480 nm, 1510 nm and 1530 nm which is around 6 and 7, respectively. At 1480 nm, 6 BS signals are generated at 50% and 60% output coupling ratio and 7 BS signals are generated at 70%, 80% and 90% output coupling ratio. At 1450 nm, 7 BS signals are generated at 70%, 80% and 90%. Meanwhile at 1530 nm, 7 BS signals are generated at 50%, 70% and 80% output coupling ratio. This condition is caused by energy inside ring cavity and gain broadening as discussed previously.

4. Conclusion

We successfully simulated and demonstrated, the MWBRFL utilizing FBG and Raman amplifier that operated in S-band wavelength region. The MWBRFL configuration consists of SMF that act as gain medium for SBS and SRS effect which is optimized by changing the output coupling ratios, RP power and tuning BP wavelength across S-band wavelength region. The Brillouin and Raman gain performance of BS signals in terms of BP wavelength, output coupling ratio and average output power are analyzed. With lower cavity loss, the reflecting FBG is utilized in the MWBRFL that to operate in the similar technique as does the reverse-S-shaped fiber section. Based on the results, the best input parameter to produce stable output BS signal is obtained at RP power of 14 dBm and BP power of 20 dBm. The MWBRFL is capable of generated 6 and 7 BS signals within wavelengths between 1480 nm and 1530 nm at 90% output coupling ratio. Meanwhile, excellent flatness average output power around 43 dBm is obtained at 90% output coupling ratio. It is significant to highlight that, the outstanding to enormous demanding on transmitting the information in fastest approach, it is necessitate expanding the communication windows into S-band wavelength region. With lower sensitivity to micro-and macrobending losses in the S-band region compared with C-band and L-band region, S-band region is higher demanding for communication system.

Acknowledgment

This work was fully supported by the Ministry of Higher Education, Malaysia under research grant # FRGS/9003-00532#. A.H. Reshak would like to acknowledge the CENTEM project, reg. no. CZ.1.05/2.1.00/03.0088, cofunded by the ERDF as part of the Ministry of Education, Youth and Sports OP RDI programme and, in the follow-up sustainability stage, supported through CENTEM PLUS (LO1402) by financial means from the Ministry of Education, Youth and Sports under the National Sustainability Programme I. Also would like to acknowledge MetaCentrum (LM2010005) and CERIT-SC (CZ.1.05/3.2.00/08.0144) infrastructures. The authors (A.H.R and Z.A.A) extend their appreciation to the International Scientific Partnership Program ISPP at King Saud University for funding this research work through ISPP# 0016.

References

[1] K.D. Park, B. Min, P. Kim, N. Park, J.H. Lee, J.S. Chang, Dynamics of cascaded Brillouin–Rayleigh scattering in a distributed fiber Raman amplifier, Opt. Lett. 27 (3) (2002) 155–157.
[2] A.K. Zamzuri, M.H. Al-Mansoori, N.M. Samsuri, M.A. Mahdi, Contribution of Rayleigh scattering on Brillouin comb line generation in Raman fiber laser, Appl. Opt. 49 (18) (2010) 3506–3510.
[3] L. Ji, H. Lee, K.J. Vahala, Low-noise Brillouin laser on a chip at 1064 nm, Opt. Lett. 39 (2) (2014) 287–290.
[4] A.K. Zamzuri, M.A. Mahdi, A. Ahmad, M.I. Md. Ali, M.H. Al-Mansoori, Flat amplitude multiwavelength Brillouin-Raman comb fiber laser in RayleighScattering-enhanced linear cavity, Opt. Express 15 (6) (2007) 3000–3005.
[5] A.H. Reshak, M.M. Shahimin, S.A.Z. Murad, S. Azizan, Simulation of Brillouin and Rayleigh scattering in distributed fibre optic for temperature and strain sensing application, Sens. Actuators A Phys. 190 (2013) 191–196.
[6] G. Mamdoohi, A.R. Sarmani, A.F. Abas, M.H. Yaacob, M. Mokhtar, M.A. Mahdi, Multi-wavelength Brillouin-Raman fiber laser utilizing enhanced nonlinear amplifying loop mirror design, Opt. Express 21 (26) (2013) 18724.
[7] M.A. Toor, N.A.M.A. Hambali, A. Mansoor, M. Ajiya, Z. Yusoff, Double Brillouin frequency shifted L-band multi-wavelength Brillouin Raman fiber laser utilizing dual laser cavity, J. Opt. 17 (2) (2015) 025502.
[8] H. Ahmad, M.Z. Zulkifli, N.A. Hassan, S.W. Harun, S-band multiwavelength ring Brillouin/Raman fiber laser with 20 GHz channel spacing, Appl. Opt. 51 (11) (2012) 1811–1815.
[9] M.Z. Zulkifli, H. Ahmad, J.M. Taib, F.D. Muhammad, K. Dimyati, S.W. Harun, S-

band multiwavelength Brillouin/Raman distributed Bragg reflector fiber lasers, Appl. Opt. 52 (16) (2013) 3753.
[10] S.R. Luthi, M.B. Costa e Silva, C.J.A. Bastos-Filho, J.F. Martins-Filho, A.S.L. Gomes, TDFA/Raman hybrid amplifiers covering the entire S-band pumped by a single laser, IEEE Photonic. Tech. Lett. 17 (10) (2005) 2050–2052.
[11] P.C. Peng, K.M. Feng, C.C. Chang, H.Y. Chiou, J.H. Chen, M.F. Huang, H.C. Chien, S. Chi, Multiwavelength fiber laser using S-band erbium-doped fiber amplifier and semiconductor optical amplifier, Opt. Comm. 259 (1) (2006) 200–203.
[12] R. Caspary, U.B. Unrau, W. Kowalsky, Recent progress on S-band fiber amplifier, in: Proc. International Conference on Transparent Optical Network, 2003.
[13] S.R. Lüthi, M.B.Ce. Silva, C.J.A. Bastos-Filho, J.F. Martins-Filho, A.S.L. Gomes, Single-pump Raman/tdfa hybrid amplifier covering the entire S-Band, IEEE Photonics Technol. Let. 17 (10) (2005) 2050–2052.
[14] Y. Liu, D. Wang, X. Dong, Stable room-temperature multi-wavelength lasing oscillations in a Brillouin–Raman fiber ring laser, Opts. Comm. 281 (21) (2008) 5400–5404.
[15] N.A.M.A.M. Hambali, H. Al-Mansoori, M. Ajiya, A.A.A. Bakar, S. Hitam, M.A. Mahdi, Multi-wavelength Brillouin-Raman ring-cavity fiber laser with 22-GHz spacing, Laser Phys. 21 (9) (2011) 1656–1660.
[16] R.W. Boyd, Nonlinear Optics, Academic Press, San Diego, 1992, p. 8.
[17] Y.G. Liu, D. Wang, X. Dong, Stable room-temperature multiwavelength lasing oscillations in a Brillouin-Raman fiber ring laser, Opt. Comm. 281 (21) (2008) 5400–5404.
[18] M. Ajiya, M.A. Mahdi, M.H. Al-Mansoori, Y.G. Shee, S. Hitam, M. Mokhtar, Reduction of stimulated Brillouin scattering threshold through pump recycling technique, Laser Phys. Lett. 6 (7) (2009) 535.
[19] M. Ajiya, M.A. Mahdi, M.H. Al-Mansoori, N.A.M.A. Hambali, S.Y. Gang, Multiwavelength Brillouin-erbium fiber laser utilizing virtual reflectivity in dispersion compensating fiber, in: IEEE, 2008 International Conference on Electronic Design, 2008, pp. 1–4.
[20] M.H. Ali, F. Abdullah, M.Z. Jamaludin, M.H. Al-Mansoori, A. Ismail, A.K. Abass, Simulation and experimental validation of gain saturation in Raman fiber amplifier, in: 3rd International Conference on Photonics, 27–29, 2012.
[21] A. Kobyakov, M. Mehendale, S. Vasilyev, Tsuda, A. Evans, Stimulated Brillouin scattering in Raman-pumped fibers: a theoretical approach, J. Light. Technol. 20 (8) (2002) 1635–1643.
[22] J.C. Haycraft, L. Stevens, Single-crystal, polarized, Raman scattering study of the molecular and lattice vibrations for the energetic material cyclotrimethylene trinitramine, Appl. Phys. 100 (2006) 053508.
[23] C. Headley, G.P. Agrawal, Raman Amplification in Fiber Optical Communication, Elsevier Academic Press, 2005.
[24] H. Zhao, S. Zhang, Spontaneous Raman scattering for simultaneous measurements of in-cylinder species, in: Third International Conference on Optical and Laser Diagnostics, 1–9, 2007.
[25] N.A.M.A. Hambali, M.A. Toor, Z. Yusoff, M. Ajiya, L-band multi-wavelength Brillouin Raman fiber laser utilizing the reverse-S-shaped section, Nonlinear Opt. Phys. 23 (2) (2014), 1450026-1–1450026-10.
[26] A.K. Ghatak, K. Thyagarajan, Optical Electronics, Cambridge University, Cambridge, 1989.
[27] J. Tang, J. Sun, L. Zhao, T. Chen, T. Huang, Y. Zhou, Tunable multiwavelength generation based on Brillouin-erbium comb fiber laser assisted by multiple four-wave mixing processes, Opt. Express 19 (15) (2009) 14682–14689.
[28] W. Al-Alimi, A. Cholan, N.A.M.H. Yaacob, M.A. Mahdi, Enhanced multiwavelength generation in Brillouin fiber laser with pump noise suppression technique, Laser Phys. 26 (2006) 065102.
[29] R.S. Shargh, M.H. Al-Mansoori, S.B.A. Anas, R.K.Z. Sahbudin, M.A. Mahdi, OSNR enhancement utilizing large effective area fiber in a multiwavelength Brillouin-Raman fiber laser, Laser Phys. Lett. 8 (2) (2010) 139–143.
[30] G.P. Agrawal, Applications of Nonlinear Fiber Optics, Academic Press, 2008.
[31] S.P. Singh, N. Singh, Nonlinear effects in optical fibers: origin, management and applications, Prog. Electromagn. Res. 73 (2007) 249–275.
[32] X. Dong, P. Shum, N.Q. Ngo, H.Y. Tam, Output power characteristics of tunable erbium-doped fiber ring lasers, J. Light. Technol. 23 (2005) 1334–1341.